

# Molecular Orientation and Field-effect Transistors of a Rigid Rod Conjugated Polymer Thin Films

Huanli Dong,<sup>†</sup> Hongxiang Li,<sup>†</sup> Erjing Wang,<sup>†</sup> Shouke Yan,<sup>\*,‡</sup> Jianming Zhang,<sup>‡</sup> Chunming Yang,<sup>§</sup> Isao Takahashi,<sup>§</sup> Hiroshi Nakashima,<sup>§</sup> Keiichi Torimitsu,<sup>§</sup> and Wenping Hu<sup>\*,†</sup>

Beijing National Laboratory for Molecular Sciences, Key Laboratory of Organic Solids and State Key Laboratory of Polymer Physics and Chemistry, Institute of Chemistry, Chinese Academy of Sciences, Beijing 100190, People's Republic of China, Department of Physics, School of Science and Technology, Kwansei Gakuin University, Sanda, Hyogo 669-1337, Japan, and NTT Basic Research Laboratories, NTT Corporation, 3-1 Morinosato Wakamiya, Atsugi, Kanagawa 243-0198, Japan

Received: December 24, 2008; Revised Manuscript Received: March 5, 2009

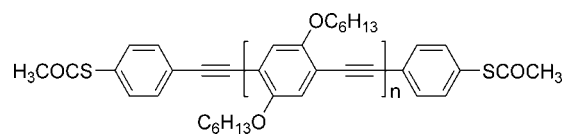
Molecular orientation in thin films of a rigid rod conjugated polymer, a derivative of poly(*para*-phenylene ethynylene)s with linear side chains and thioacetyl end groups, was investigated by reflection–absorption infrared spectroscopy and X-ray diffraction technique. The results indicated that TA-PPE molecules tended to align with their backbone planes perpendicular to substrates, that is, with an “edge-on” molecular orientation in the films. Such molecular orientation is favorable for the efficient carrier transport in two-dimensional direction in the polymer films (i.e., via both the intrachain and interchain), so that high performance organic field-effect transistors were fabricated with hole mobility at around  $\sim 4.3 \times 10^{-3} \text{ cm}^2/\text{Vs}$ .

## 1. Introduction

Conjugated polymers are of great interest in light-emitting diodes, photovoltaic cells, transistors, and so forth due to their excellent optoelectronic, low-cost, and nice solution-processed properties.<sup>1–5</sup> The performance of the devices is determined not only by the structure of the polymers, but also by the molecular orientation in the films.<sup>6–10</sup> It is well known that highly ordered molecular structure is efficient for charge transport and beneficial for the achievement of high carrier mobility. Moreover, molecular alignment with respect to substrates in thin films is also decided by device configuration. For example, in sandwiched organic photovoltaic devices the molecules in films are hoped to be parallel to the substrates,<sup>11,12</sup> while in organic field-effect transistors (OFETs) the molecules had better organize themselves with their backbone planes being perpendicular to the substrates.<sup>13–15</sup> Thus, molecular orientation in thin films plays a key role in determining the charge transport mechanisms and rationally optimizing the device configuration for further improvement of the device performance.

Poly(*para*-phenylene ethynylene)s (PPEs), an important class of conjugated polymer materials, exhibit not only excellent optoelectronic properties but also high thermal and oxidative properties, as well as photostability and ideal rigidity, which make them attractive in many research fields, such as fluorescent chemical sensors, molecular electronics, photonic and optoelec-

## SCHEME 1: Molecular Structure of TA-PPE



tronic devices, and so forth.<sup>16–21</sup> Although the performance of these devices is strongly influenced by the polymer solid-state structure, until now the detailed structural information of PPEs is rarely addressed. Some reports in the literature have shown that the PPE derivatives with linear side chains generally prefer to form highly ordered supramolecular architectures in the solid state, where the rigid bulk chains are oriented coplanar, and the linear side chains extend laterally within the plane of their respective chains in interdigitated or tiled form.<sup>22–26</sup> However, in these cases how the molecules align with respect to the substrates that have direct influence on the physical properties of devices<sup>13–15</sup> has not been fully understood, except for their behavior in solution.<sup>27,28</sup> Moreover, up until now no report has addressed the applications of PPEs in OFETs, although their semiconducting properties have received much attentions for decades.<sup>22,29,30</sup> Evoked by these considerations, here a derivative of PPEs with linear alkoxy side chains and thioacetyl end groups (TA-PPE, Scheme 1) is used as an example<sup>31–36</sup> to investigate the molecular orientation in TA-PPE thin films by using the grazing incidence X-ray diffraction (GIXD) technique and reflection–absorption infrared (RAIR) spectroscopy. Then, OFETs with the TA-PPE thin films as active layers were fabricated to demonstrate their field-effect performance. The structure of the TA-PPE films, the preferential orientation of the polymer chains in the films, the field-effect transistors, and mobility of the polymer are examined for the first time here.

\* To whom correspondence should be addressed. E-mail: (S.Y.) skyan@iccas.ac.cn; (W.H.) huwp@iccas.ac.cn.

<sup>†</sup> Key Laboratory of Organic Solids, Chinese Academy of Sciences.

<sup>‡</sup> State Key Laboratory of Polymer Physics and Chemistry, Chinese Academy of Sciences.

<sup>§</sup> Kwansei Gakuin University.

<sup>§</sup> NTT Corporation.

The key issues are believed to be attractive and important for the potential applications of the polymer in organic/plastic electronics.

## 2. Experimental Section

TA-PPE was synthesized through Sonogashira Pd–Cu coupling reaction as described elsewhere.<sup>37,38</sup> The molecular weight (Mw) of our TA-PPE was about 51 328 g/mol with a polydispersity (*D*) of 3.09, which was estimated by gel permeation chromatography (GPC) with polystyrene as calibration standard and tetrahydrofuran (THF) as the eluent at room temperature. About 5 mg/mL chlorobenzene solution was prepared and drop-cast onto the substrates with slow evaporation in a closed jar. The thickness of the films was about 70–100 nm measured by Ambios Technology XP-2 profilometer and all the TA-PPE films were dried in a vacuum oven at 60 °C for 4 h to remove the residual solvent prior to measurement.

The substrates used in the present study were successively cleaned with pure water, hot concentrated sulfuric acid–hydrogen peroxide solution (concentrated sulfuric acid/hydrogen peroxide water = 2:1), pure water, pure ethanol, and pure acetone. A self-assembled monolayer (SAM) of trichloro(octadecyl)silane (OTS) was produced on the Si/SiO<sub>2</sub> wafer surfaces using a normal vapor deposition method described elsewhere.<sup>39</sup> Top-contacted OFETs based on the drop-cast TA-PPE films were constructed on the OTS-modified Si/SiO<sub>2</sub> substrates (n-type Si wafer with 500 nm thick SiO<sub>2</sub>, capacitance = 7.5 nF/cm<sup>2</sup>). Subsequently, 30 nm thick source and drain electrodes of the transistors were deposited via a shadow mask on the polymer thin films. The channel length and width of the transistors were 0.02 and 0.15 mm, respectively.

*I*–*V* characteristics of OFETs were recorded by a Keithley 4200 SCS with a Micromanipulator 6150 probe station in a clean and shielded box at room temperature in air. X-ray diffraction (XRD) was measured on D/max2500 by the usual  $\theta$ – $2\theta$  method with 40 kV voltage and a Cu K $\alpha$  source ( $\lambda$  = 1.541 Å). Grazing incidence X-ray diffraction (GIXD) measurement was performed by a four-circle diffractometer (SMARTLAB, Rigaku Co.) with a rotating Cu anode X-ray generator. The incidence angle was fixed at 0.3° so that the X-ray beam could penetrate the entire thickness of the film samples (~100 nm). Reflection–absorption infrared (RAIR) and transmission infrared (TIR) were recorded via a Bruker EQUINOX 55 Fourier transform infrared spectrometer with a DTGS detector. The measurements were carried out at a resolution of 4 cm<sup>−1</sup> by averaging 32 scans. For RAIR measurements, the incidence angle was fixed at 83° for the best signal recording. Atomic force microscopy (AFM) measurement was carried out with Nanoscope IIIa (USA) in a tapping model.

## 3. Results and Discussion

Figure 1a shows the XRD patterns of TA-PPE films (thickness is around 2  $\mu$ m) peeled off from substrates. It is obvious that there are two typical diffraction peaks at  $2\theta$  = 6.20° and 22.10°, which suggests the formation of typical lamellar structure in the solid state of TA-PPE polymer and is similar to those PPE derivatives with linear side chains.<sup>22–26</sup> According to literature,<sup>22–26</sup> the primary peak at  $2\theta$  = 6.20° arises from the ordered interlayer stacking of the polymers and corresponds to an interlayer *d*-spacing of 14.2 Å separated by the hexyloxy side groups, while the wide-angle peak at 22.10° with *d*-spacing of 4.0 Å is attributed to the  $\pi$ – $\pi$  interchain stacking of adjacent conjugated polymer main chains, as depicted in the inset of Figure 1a. The sharpness and intensity of the first-order reflection (*d* = 14.2 Å) points to an appreciable degree of side

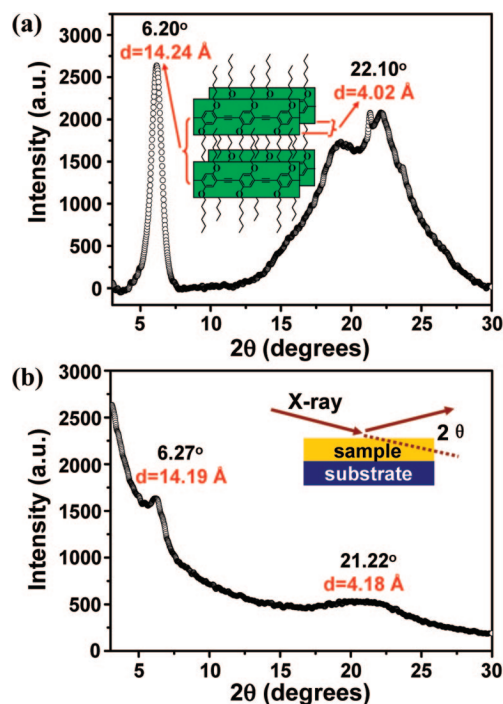


**Figure 1.** (a) XRD pattern of multiple drop-cast TA-PPE films peeled off from the substrate. (b) Out-of-plane GIXD profile of the thin drop-cast TA-PPE films on OTS-modified substrates (incidence angle fixed at 0.3°). The inset shows the schematic representation of out-of-plane GIXD measurement.

chain crystallinity with a long-range order. This well-defined layered structure assumes two possible molecular orientations in the films, that is, “face-on” lamellar orientation and “edge-on” lamellar orientation. To investigate the preferred orientation of TA-PPE molecules in the solid state, GIXD measurement was performed on the thin drop-cast TA-PPE films on OTS-modified Si/SiO<sub>2</sub> substrate, as displayed in Figure 1b. Comparing with the XRD patterns of TA-PPE films (Figure 1a), the peak at  $2\theta$  = 22.10° corresponding to the  $\pi$ -stack distance became very weak (Figure 1b) and the intensity ratio of peaks at 6.20° to 22.10° increased from 1.2 (in Figure 1a) to 3.2 (in Figure 1b), indicating the preferable “edge-on” molecular orientation in the thin drop-cast TA-PPE films because of the ability of out-of-plane GIXD measurement to give peaks with respect to the substrate in depth of the films. Moreover, the temperature dependence of the in situ out-of-plane GIXD profiles further confirmed the molecular orientation in TA-PPE films. With the annealing temperature increasing (from room temperature to 150 °C), the peak at  $2\theta$  = 6.27° corresponding to the interlayer spacing was obviously increased (see Supporting Information), that is, the annealing process definitely preferred “edge-on” molecular orientation in TA-PPE films. Therefore, it is reasonable to deduce that higher molecular orientation films could be obtained by precisely controlling the sample preparation and annealing process.

Additionally, the orientation of TA-PPE molecules in the thin films was further investigated by using the convenient RAIR spectroscopy, which is sensitive to the vibration modes and independent of the crystalline degree of the films, thus RAIR can be used as a combined method for the GIXD technique in exploring the molecular orientation of thin films.<sup>40</sup> Compared to TIR spectrum, in RAIR spectrum by producing an electrical field vector perpendicular to the surface, the intensity of those vibration modes with transition moments perpendicular to the surface would be obviously enhanced and the intensity of those

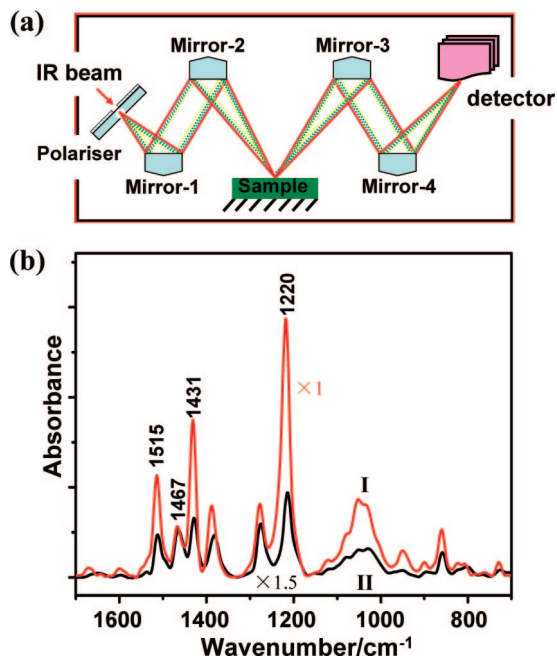


**Figure 2.** (a) Schematic diagram of RAIR measurement. (b) Comparison of RAIR (I) and TIR (II) spectra of the thin drop-cast TA-PPE films.

modes having transition moment parallel to the substrate would be lowered.<sup>40,41</sup> Figure 2a shows the schematic diagram of RAIR measurement and Figure 2b gives the comparison of RAIR and TIR spectra of the thin drop-cast TA-PPE films. Thereinto, the assignment of some characteristic IR bands of TA-PPE is summarized in Table S1 (see Supporting Information).<sup>42,43</sup> The band at  $1467\text{ cm}^{-1}$  assigned to the  $\text{CH}_2$  deformation vibration could be used as the reference in this case because it originates from the flexible side chains and exhibits no defined polarization with respect to the substrates. Detailed information for the corresponding relative intensity ratios of the peaks in RAIR and TIR is demonstrated in Table S2 (see Supporting Information). It is obvious that the RAIR bands at  $1515$ ,  $1431$ , and  $1220\text{ cm}^{-1}$  are significantly increased compared to those of TIR. Considering the fact that the bands at  $1515$  and  $1431\text{ cm}^{-1}$  come from the in-plane-stretching vibrations of  $\text{C}=\text{C}$  in phenyl rings,<sup>42,43</sup> it can be concluded that the TA-PPE molecules tend to align with the phenyl ring planes perpendicular to the substrate. It is further confirmed by the peak at  $1220\text{ cm}^{-1}$  of the stretching vibration of  $\text{Ph}-\text{O}-\text{C}$ ,<sup>42,43</sup> which also exhibits obvious increase in the RAIR spectrum due to the  $\text{Ph}-\text{O}-\text{C}$  vibration preferentially perpendicular to the substrate plane. Therefore, taking all above analyses into consideration, the present RAIR results suggest that the TA-PPE molecules generally prefer to be aligned with the phenyl ring plane perpendicular to the substrate in the thin drop-cast films, that is, “edge-on” molecular orientation, which further confirms the results derived from the GIXD measurement (Figure 1b). Such preferable “edge-on” molecular orientation in TA-PPE thin films should be advantageous for the fabrication of OFETs, because of the efficient two-dimensional charge carrier transport (via both the intrachain and interchain directions) in the polymer thin films.<sup>13–15</sup>

Molecular orientation in thin films is critical for determining charge transport. However, other factors possibly influencing the performance of devices are the morphology of thin films (e.g., surface roughness, grain sizes, and so forth)<sup>8–10</sup> and the interface properties between polymer semiconductor and gate insulator. As shown in Figure 3a,b, the AFM topographic images of

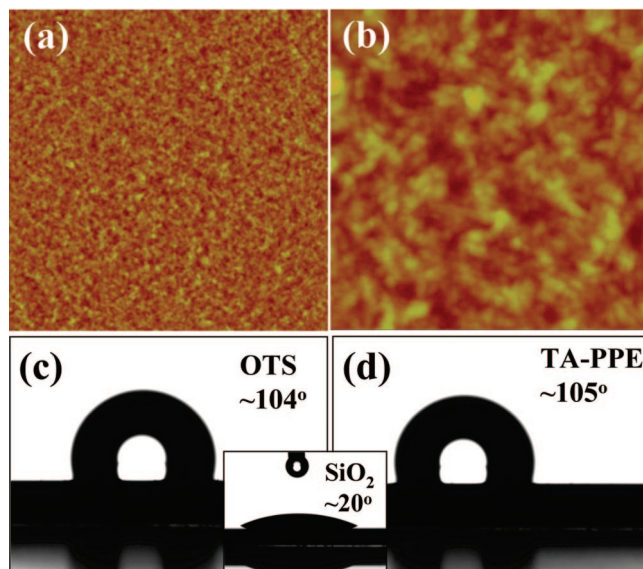


**Figure 3.** AFM topographic images of the thin drop-cast TA-PPE films on OTS-modified Si/SiO<sub>2</sub> substrate with image size of (a)  $5 \times 5\text{ }\mu\text{m}^2$  and (b)  $1 \times 1\text{ }\mu\text{m}^2$ , respectively, (c) Water contact angle measurement, and the water contact angle on SiO<sub>2</sub> (inset), SiO<sub>2</sub>–OTS (c) and TA-PPE (d) surfaces. The contact angles between SiO<sub>2</sub>–OTS and TA-PPE are highly identical, indicating the intimate contact, that is, the compatible interfaces for polymer transistors.

of TA-PPE films on OTS-modified Si/SiO<sub>2</sub> substrates show a homogeneous morphology with granule crystallite ( $\sim 100\text{ nm}$ ) and a smooth surface with low root-mean-square (rms) roughness of about  $2\text{--}4\text{ nm}$ . The results confirm the good quality of TA-PPE films for the potential fabrication of devices.

In polymer transistors the conduction channel locates accurately at the interface between polymer semiconductor layer and gate insulator. So, the interface, especially the contact intimacy between the polymer semiconductor and gate insulator, plays a critical role for the performance of polymer transistors. As described by Li et al.<sup>44</sup> the wettability is a simple and useful parameter to evaluate the surface contact intimacy of heterogeneous surfaces. Only the surfaces with similar hydrophobicity or hydrophilicity can adhere to each other intimately according to the surface “compatibility and similitude principle”.<sup>44</sup> In our polymer devices here, two interfaces (the contacts of SiO<sub>2</sub>/TA-PPE and OTS/TA-PPE) are very important for the transistors. The wettability of the three surfaces (SiO<sub>2</sub>, SiO<sub>2</sub>–OTS, and TA-PPE) examined by their water CAs are  $\sim 20^\circ$ ,  $104^\circ$ , and  $105^\circ$ , respectively (Figure 3c,d). The contact angles between SiO<sub>2</sub>–OTS and TA-PPE were highly identical, indicating the necessity of the OTS modification and the intimate contact of the interface between the polymer semiconductor and gate insulator for high performance transistors.

To validate the transport properties of TA-PPE films, top-contact OFETs (Figure 4a) based on the thin drop-cast TA-PPE films are fabricated on OTS-modified Si/SiO<sub>2</sub> substrate (the back low resistance Si as gate and SiO<sub>2</sub> (500 nm) as gate insulator) and are measured in air at room temperature. In the domains of the films, the molecular orientation of TA-PPE is depicted by Figure 4b. The corresponding output and transfer characteristics of the OFETs are shown in Figure 4c,d. These devices exactly exhibit typical *p*-type field-effect modulation characteristics. The field-effect mobility ( $\mu$ ) in the saturated region and threshold voltage ( $V_T$ ) could be calculated using the following equation:<sup>45</sup>



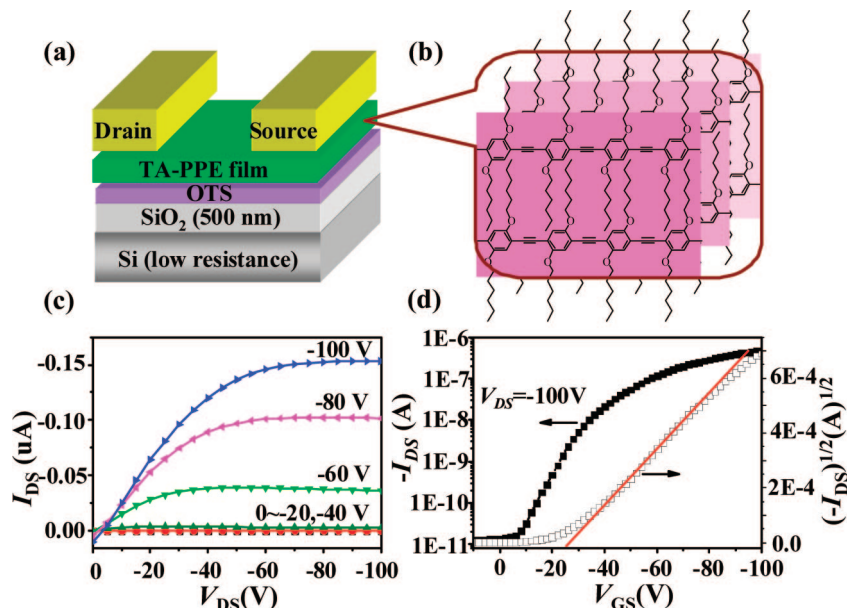


**Figure 4.** (a) Schematic bottom-gate, top-contact OFETs geometry on OTS-modified Si/SiO<sub>2</sub> substrates. (b) Representative “edge-on” molecular orientation in TA-PPE films suggested above. (c) Output and (d) transfer characteristics of an exemplary TA-PPE thin film OFET. The corresponding saturated field-effect mobility, on/off ratio, and threshold voltage ( $V_T$ ) of this device were estimated at around  $4.3 \times 10^{-3} \text{ cm}^2/\text{Vs}$ ,  $3.8 \times 10^4$ , and  $-28 \text{ V}$ , respectively.

$$I_{DS, \text{sat}} = \frac{WC_i}{2L} \mu_{\text{sat}} (V_{GS} - V_T)^2 \quad (1)$$

where  $W$  and  $L$  are the channel width and length, respectively,  $C_i$  is the capacitance per unit area of the gate insulator,  $\mu_{\text{sat}}$  is the field-effect mobility in the saturated region,  $V_{GS}$  is the gate voltage, and  $V_T$  is the threshold voltage. The corresponding saturated field-effect mobility, on/off ratio, and threshold voltage are estimated at around  $4.3 \times 10^{-3} \text{ cm}^2/\text{Vs}$ ,  $3.8 \times 10^4$ , and  $-28 \text{ V}$ , respectively. To our knowledge, it is the first time for the application of PPE derivatives in OFETs, and they definitely exhibit good field-effect performance due to the favorable molecular orientation in the thin films with efficient charge carrier transport. Moreover, it is believed that much higher device performance could be obtained along with the reduction of charge injection barriers between Au electrode (work function at  $\sim 5.2 \text{ eV}$ ) and the TA-PPE molecules (HOMO energy locating at  $\sim 6.3 \text{ eV}$ )<sup>16</sup> by virtue of the thioacetyl end groups.<sup>18,46,47</sup>

#### 4. Conclusions

In conclusion, the molecular orientation of a rigid rod conjugated polymer (TA-PPE) in thin drop-cast films was investigated by X-ray diffraction technique and reflection-absorption infrared. The results indicated that TA-PPE molecules tended to align with their backbone planes perpendicular to the substrate, that is, “edge-on” molecular orientation in the films. OFETs based on the TA-PPE films exhibited good field-effect performance with carrier mobility of  $4.3 \times 10^{-3} \text{ cm}^2/\text{Vs}$ , probably due to the efficient charge transport in two-dimensional direction (via both the intrachain and interchain directions) in the polymer films.

**Acknowledgment.** The authors thank the financial support from National Natural Science Foundation of China (20721061, 50725311, 60736004, 60771031), Ministry of Science and Technology of China (2006CB806200, 2006CB932100), and Chinese Academy of Sciences.

**Supporting Information Available:** Supplementary Tables for some characteristic IR bands of TA-PPE in situ out-of-plane

GIXD profiles of the thin drop-cast TA-PPE films under different annealed temperatures. This material is available free of charge via the Internet at <http://pubs.acs.org>.

#### References and Notes

- (1) Skotheim, T. A. *Handbook of Conducting Polymers*, 2nd ed.; Marcel Dekker, New York, 1986; Vols. 1 and 2.
- (2) *Conjugated Conducting Polymers*; Kiess, H. G., Ed.; Springer-Verlag: Berlin, 1992.
- (3) Reese, C.; Roberts, M.; Ling, M.-M.; Bao, Z. *Mater. Today* **2004**, 7, 20.
- (4) Forrest, S. R. *Nature* **2004**, 428, 911.
- (5) Sirringhaus, H.; Kawase, T.; Friend, R. H.; Shimoda, T.; Inbasekaran, M.; Wu, W.; Woo, E. P. *Science* **2000**, 290, 2123.
- (6) Ziegler, C. In *Handbook of Organic Conductive Molecules and Polymers*; Nalwa, H. S., Ed.; Wiley: Chichester, U.K., 1997; Vol. 3, Chapter 13.
- (7) Scherf, U.; List, E. J. W. *Adv. Mater.* **2002**, 14, 477.
- (8) McCulloch, I.; Heeney, M.; Bailey, C.; Genevicius, K.; Macdonald, I.; Shkunov, M.; Sparrowe, D.; Tierney, S.; Wagner, R.; Zhang, W.; Chabinyc, M. L.; Kline, R. J.; McGehee, M. D.; Toney, M. F. *Nat. Mater.* **2006**, 5, 328.
- (9) Wu, Y.; Liu, P.; Ong, B. S.; Srikumar, T.; Zhao, N.; Botton, G.; Zhu, S. *Appl. Phys. Lett.* **2005**, 86, 142102.
- (10) Li, G.; Shrotriya, V.; Huang, J.; Yao, Y.; Moriarty, T.; Emery, K.; Yang, Y. *Nat. Mater.* **2005**, 4, 864.
- (11) Tang, C. W. *Appl. Phys. Lett.* **1986**, 48, 183.
- (12) Yang, F.; Shtein, M.; Forrest, S. R. *Nat. Mater.* **2005**, 4, 37.
- (13) Sirringhaus, H.; Brown, P. J.; Friend, R. H.; Nielsen, M. M.; Bechgaard, K.; Langeveld-Voss, B. M. W.; Spiering, A. J. H.; Janssen, R. A. J.; Meijer, E. W.; Herwig, P.; de Leeuw, D. M. *Nature* **1999**, 401, 685.
- (14) Kim, D. H.; Park, Y. D.; Jang, Y.; Yang, H.; Kim, Y. H.; Han, J. I.; Moon, D. G.; Park, S.; Chang, T.; Chang, C.; Joo, M.; Ryu, C. Y.; Cho, K. *Adv. Funct. Mater.* **2005**, 15, 77.
- (15) Lan, Y. K.; Huang, C. I. *J. Phys. Chem. B* **2008**, 112, 14857.
- (16) Bunz, U. H. F. *Chem. Rev.* **2000**, 100, 1605.
- (17) McQuade, D. T.; Pullen, A. E.; Swager, T. M. *Chem. Rev.* **2000**, 100, 2537.
- (18) Tour, J. M. *Acc. Chem. Res.* **2000**, 33, 791.
- (19) Schmitz, C.; Pösch, P.; Thelakkat, M.; Schmidt, H.-W.; Montali, A.; Feldman, K.; Smith, P.; Weder, C. *Adv. Funct. Mater.* **2001**, 11, 41.
- (20) Pschirer, N. G.; Miteva, T.; Evans, U.; Roberts, R. S.; Marshall, A. R.; Neher, D.; Myrick, M. L.; Bunz, U. H. F. *Chem. Mater.* **2001**, 13, 2691.
- (21) Xu, Y.; Berger, P. R.; Wilson, J. N.; Bunz, U. H. F. *Appl. Phys. Lett.* **2004**, 85, 4219.

- (22) Bunz, U. H. F.; Enkelmann, V.; Kloppenburg, L.; Jones, D.; Shimizu, K. D.; Claridge, J. B.; zur Loye, H.-C.; Lieser, G. *Chem. Mater.* **1999**, *11*, 1416.
- (23) Weder, C.; Wrighton, M. S. *Macromolecules* **1996**, *29*, 5157.
- (24) Ofer, D.; Swager, T. M.; Wrighton, M. S. *Chem. Mater.* **1995**, *7*, 418.
- (25) Li, H.; Powell, D. R.; Hayashi, R. K.; West, R. *Macromolecules* **1998**, *31*, 52.
- (26) Weder, C.; Wrighton, M. S.; Spreiter, R.; Bosshard, C.; Günter, P. *J. Phys. Chem.* **1996**, *100*, 18931.
- (27) Miteva, T.; Palmer, L.; Kloppenburg, L.; Neher, D.; Bunz, U. H. F. *Macromolecules* **2000**, *33*, 652.
- (28) Kim, J.; Swager, T. M. *Nature* **2001**, *411*, 1030.
- (29) Kokil, A.; Shiyanovskaya, I.; Singer, K. D.; Weder, C. *Synth. Met.* **2003**, *138*, 513.
- (30) Kokil, A.; Shiyanovskaya, I.; Singer, K. D.; Weder, C. *J. Am. Chem. Soc.* **2002**, *124*, 9978.
- (31) Hu, W.; Nakashima, H.; Furukawa, K.; Kashimura, Y.; Ajito, K.; Torimitsu, K. *Appl. Phys. Lett.* **2004**, *85*, 115.
- (32) Hu, W.; Nakashima, H.; Furukawa, K.; Kashimura, Y.; Ajito, K.; Liu, Y.; Zhu, D.; Torimitsu, K. *J. Am. Chem. Soc.* **2005**, *127*, 2804.
- (33) Hu, W.; Jiang, H.; Nakashima, H.; Luo, Y.; Kashimura, Y.; Chen, K.; Shuai, Z.; Furukawa, K.; Lu, W.; Liu, Y.; Zhu, D.; Torimitsu, K. *Phys. Rev. Lett.* **2006**, *96*, 027801.
- (34) Hu, W.; Nakashima, H.; Furukawa, K.; Kashimura, Y.; Ajito, K.; Han, C.; Torimitsu, K. *Phys. Rev. B* **2004**, *69*, 165207.
- (35) Hu, W.; Nakashima, H.; Wang, E.; Furukawa, K.; Li, H.; Luo, Y.; Shuai, Z.; Kashimura, Y.; Liu, Y.; Torimitsu, K. *Pure Appl. Chem.* **2006**, *78*, 1803.
- (36) Dong, H.; Li, H.; Wang, E.; Wei, Z.; Xu, W.; Hu, W.; Yan, S. *Langmuir* **2008**, *24*, 13241.
- (37) Nakashima, H.; Furukawa, K.; Kashimura, Y.; Torimitsu, K. *Polym. Prepr.* **2003**, *44*, 482.
- (38) Nakashima, H.; Furukawa, K.; Ajito, K.; Kashimura, Y.; Torimitsu, K. *Langmuir* **2005**, *21*, 511.
- (39) Li, L.; Tang, Q.; Li, H.; Yang, X.; Hu, W.; Song, Y.; Shuai, Z.; Xu, W.; Liu, Y.; Zhu, D. *Adv. Mater.* **2007**, *19*, 2613.
- (40) Zhang, Y.; Mukoyama, S.; Hu, Y.; Yan, C.; Ozaki, Y.; Takahashi, I. *Macromolecules* **2007**, *40*, 4009.
- (41) Wang, J.; Shen, D.; Yan, S. *Macromolecules* **2004**, *37*, 8171.
- (42) Lin-Vien, D.; Colthup, N. B.; Fateley, W. G.; Grasselli, J. G. *Handbook of Infrared and Raman Characteristic Frequencies of Organic Molecules*; Academic Press Inc.: San Diego, CA, 1991.
- (43) Nakashima, K.; Ren, Y.; Nishioka, T.; Tsubahara, N.; Noda, I.; Ozaki, Y. *J. Phys. Chem. B* **1999**, *103*, 6704.
- (44) Li, L.; Tang, Q.; Li, H.; Hu, W. *J. Phys. Chem. B* **2008**, *112*, 10405.
- (45) Sze, S. M. *Physics of Semiconductor Devices*, 2nd ed.; Wiley: New York, 1981.
- (46) Zangmeister, C. D.; Picraux, L. B.; van Zee, R. D.; Yao, Y.; Tour, J. M. *Chem. Phys. Lett.* **2007**, *442*, 390.
- (47) Zangmeister, C. D.; Robey, S. W.; van Zee, R. D.; Yao, Y.; Tour, J. M. *J. Phys. Chem. B* **2004**, *108*, 16187.

JP811374H